



The Open Construction and Building Technology Journal

Content list available at: www.benthamopen.com/TOBCTJ/

DOI: 10.2174/1874836801610010466



RESEARCH ARTICLE

Parametric Analysis on Collapse-resistance Performance of Reinforced-concrete Frame with Specially Shaped Columns Under Loss of a Corner Column

Lei Zhang¹, Hailong Zhao^{1,2,*}, Tiecheng Wang^{1,2} and Qingwei Chen¹

¹School of Civil Engineering, Tianjin University, Tianjin, P.R. China

²Key Laboratory of Coast Civil Structures, Tianjin University, Ministry of Education, Tianjin, P.R. China

Received: January 27, 2016

Revised: June 02, 2016

Accepted: June 03, 2016

Abstract: A finite element model is verified accurate enough to simulate the static test of one reinforced-concrete frame with specially shaped columns subjected to the loss of a ground corner column. As the frame sustained loads primarily depending on the beam resisting mechanism in the test, four related parameters, namely the height of beam section, rebar ratio of beam, rebar ratio of slab and limb length of specially shaped column are chosen for parametric analyses respectively. It is indicated that the collapse-resistance capacity remarkably increases with the increasing of the height of beam section and rebar ratio of the lower steel bars of beam. The increase of the rebar ratio of slab and upper steel bars of beam could enhance the stiffness and collapse-resistance capacity slightly. The lengthening of the limb of specially shaped column only increases the stiffness of the frame. According to an equivalent method, the rectangular column frame is obtained to compare collapse-resistance performance with the specially shaped column frame. It is concluded that the frame with specially shaped columns could maintain the equivalent collapse-resistance capacity while reduce the lateral stiffness compared with the rectangular column frame.

Keywords: Alternate path analysis, Column failure, Nonlinear analysis, Parametric analysis, Progressive collapse and specially shaped column.

1. INTRODUCTION

Progressive collapse is defined as the spread of an initial local failure from element to element, which eventually results in the collapse of an entire structure or a disproportionately large part of it [1]. Since the Ronan Point apartment building collapse in England in 1968, many design guidelines [2, 3] have been proposed to assess progressive collapse potential of the structure subjected to the loss of columns. Meanwhile, many experimental and numerical studies have been carried out in terms of progressive collapse issue. Sasaki *et al.* [4] used experimental and analytical results to evaluate the collapse-resistance capacity of an actual RC structure and identified the development of Vierendeel action as the dominant mechanism in redistribution of loads in the structure. Izzuddin *et al.* [5] assessed the potential of multi-storey buildings considering sudden column loss as a design scenario through a new method, which offers for the first time a quantitative framework for the consideration of such important issues as ductility, redundancy and energy absorption. Yi *et al.* [6] performed a static test on a planar frame to investigate the collapse process. The results indicated that the test model went through three stages (*i.e.* elastic, plastic and catenary stages). Su *et al.* [7] carried out an experimental study to look into the load-carrying capacity of RC frame beams when a supporting column is failed to work. The tests confirmed the strength enhancement effect of compressive arch action on beam flexural capacity. Lew *et al.* [8] conducted full-scale testing of two steel-beam column assemblies, each comprising three columns and two beams and representing part of the second-floor framing of a 10-story steel frame building. The test results indicated

* Address correspondence to this author at School of Civil Engineering, Tianjin University, 300072, Tianjin, P.R. China; Tel: (+86) 13821290260; E-mails: hgtdtkimi@163.com, zhao_hailong@126.com

that the rotational capacities of both connections under monotonic column displacement are about twice as large as those based on seismic-test data. Guo *et al.* [9] conducted an experimental study of a steel-concrete composite frame with rigid connections. The study indicated that collapse mechanism of composite frame consisted of six stages including elastic, elastic-plastic, arch, plastic, transient and catenary stages; and the catenary action could enhance the resistance of rigid composite frame evidently. Rahai *et al.* [10] addressed progressive collapse in a five-story reinforced concrete building model resulting from gradual removal of columns due to fire propagation in a specific zone of structure and compared the results with the findings in the scenario of instantaneous removal of column. Xiao *et al.* [11] conducted three tests of a three-bay x three-bay, three-story and half-scale RC frame following a series of sudden column removals. The results indicated that the structure did not collapse in the scenario of corner or inner column removal, but experienced transition from moment resisting mechanism to catenary mechanism in the scenario of two side columns removal. Wang *et al.* [12] investigated the dynamic response of a six-story frame caused by employing the nonlinear dynamic methodology. The results indicated that the internal force redistribution mainly appeared in the components adjacent to the failure column and the model had the worst capacity to resist progressive collapse in the inner column demolition scenario. Palmisano [13] found that the activation of the elasto-plastic catenary behavior of the slab reinforcement could be very effective to increase the building robustness without substantially increasing the cost of a structural system. Wang *et al.* [14, 15] performed collapse experiments on the RC frame with specially shaped columns subjected to middle and corner column removal respectively. The results revealed that the redistribution of internal force was mainly realized through the beam mechanism and the compressive arch action played an important role to improve the collapse-resistant capacity.

It can be seen from the above studies that they were focused on the studies of rectangular column frames. Few literature paid attention to the progressive collapse potential of reinforced concrete frames with specially shaped columns, which can offer advantages such as avoiding prominent corners in a room and increasing usable floor area so as to be widely applied in multistoried and high-rise buildings in China. Thus, it is necessary to further study the collapse-resistance performance of the frame with specially shaped columns due to its particular section properties. A static test of a RC frame with specially shaped columns following the removal of a ground corner column is described and discussed in this paper. Furthermore, a finite element model was developed to compare with the test results. To study the factors affecting the collapse-resistance performance, four various parameters were chosen for parametric analyses. Then specially shaped columns were equivalent to rectangular columns to compare the behaviors of the two frames.

2. COLLAPSE-RESISTANCE TEST

2.1. Overview of Test

To study the progressive collapse potential of RC frames with specially shaped columns following the loss of a ground corner column, an experiment of a one-third scale, two-bay x three-bay, two-story model frame was carried out as shown in Fig. (1) [14]. The dimensions of the model frame and measuring points are displayed in Fig. (2). The height of story was 1m, and the thickness of slab was designed as 50mm. C8 steel bars were orthogonally allocated inside the slab with the interval of 150mm. The section dimensions and reinforcements of columns and beams are displayed in Fig. (3). The reinforcement details of beam-column joints are provided in Fig. (4), in which longitudinal reinforcements of beams and columns passed through joints. The grade of steel bars in beams and columns is HRB400 for the main reinforcements and HPB300 for the stirrups. The grade of steel bars in slabs is HRB400. The material properties of steel are listed in Table 1, where f_y , f_u , δ and E_s are steel yield strength, ultimate strength, ratio of elongation and elastic modulus. The average compressive strength of concrete is 42.3 MPa, which is obtained from standard 150 mm cubes. The complete stress-strain curves of concrete are displayed in Fig. (5), which are obtained from 150 mm x 150 mm x 300 mm prismoids. The ground column A4 designed as the failed column was substituted by a steel pipe to support the superstructure during the concrete casting process. After the maintenance of the model frame, sandbags were uniformly placed on slabs with 2.8kN/m² load applied. The vertical load in succession was applied by a 1000 kN hydraulic jack installed on top of second-floor column A4 to perform a static test. Fig. (6) depicts the details of the loading equipment in the test. The load and displacement-controlled manner was applied in the loading process. Fig. (7) shows the relationship of the force applied by the jack *versus* the downward displacement on top of the failed corner column. It is indicated that the collapse process consists of four distinct phases: elastic phase (OA), elasto-plastic phase (AB), plastic-hinge phase (BD) and collapse phase (DE). It is worth noting that the measured force reached its peak value of 152.8 kN at Point C.



Fig. (1). Experimental set-up.

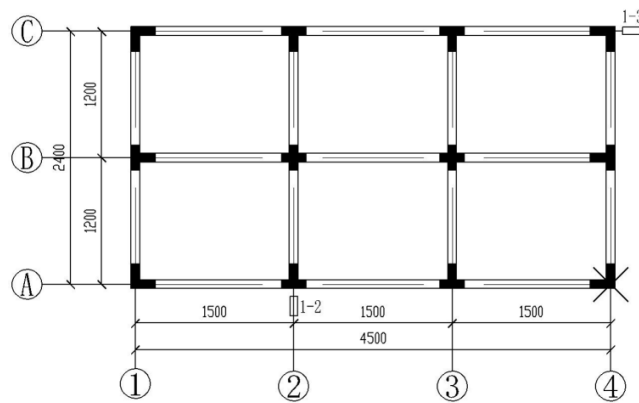


Fig. (2). First-floor plan (dimensions in mm).

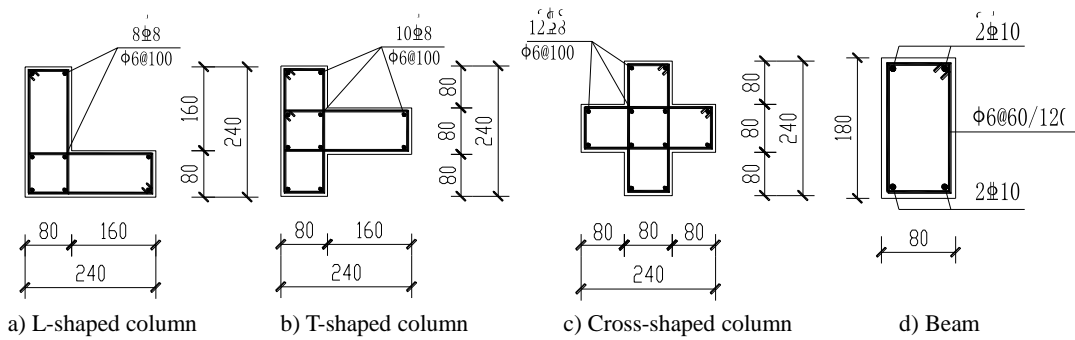


Fig. (3). Section details (dimensions in mm).

(Note: A and C stand for steel strength grade of HPB300 and HRB400 in Chinese concrete code respectively. @ stands for stirrup space. There is a decrease in spacing of beam stirrup by half of the above near beam-column joint.)

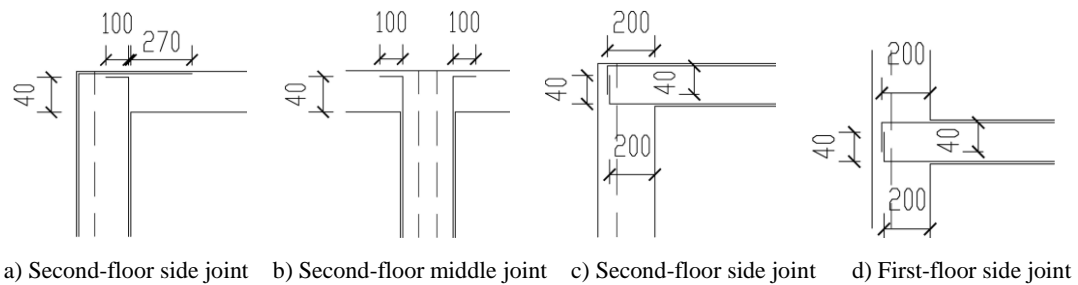


Fig. (4). Reinforcement details of beam-column joints (dimensions in mm).

Table 1. Mechanical properties of steel.

Reinforcement	f_y /MPa	f_u /MPa	δ /%	E_s /(10 ⁵ MPa)
A6	417.0	541.4	30.4	2.12
C8	454.1	640.3	28.4	2.65
C10	433.6	627.8	29.1	2.25

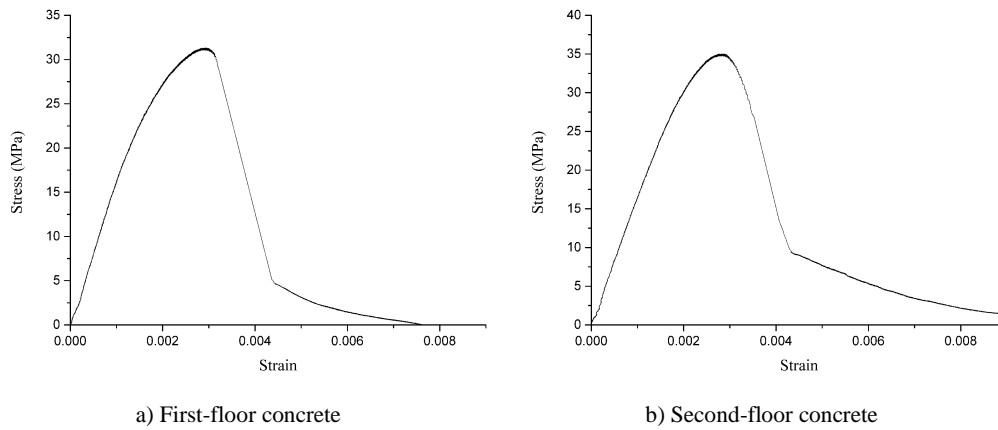


Fig. (5). Stress-strain curves of concrete.

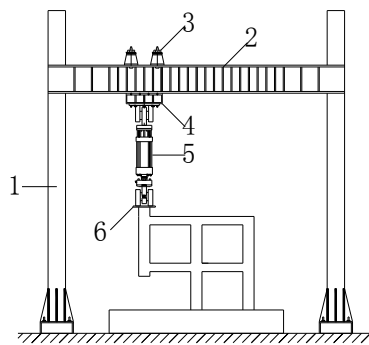


Fig. (6). Loading equipment. Note: 1. Column; 2. Load-carrying beam; 3. Girder; 4. Box-girder; 5. Hydraulic jack; 6. Inserted steel plate.

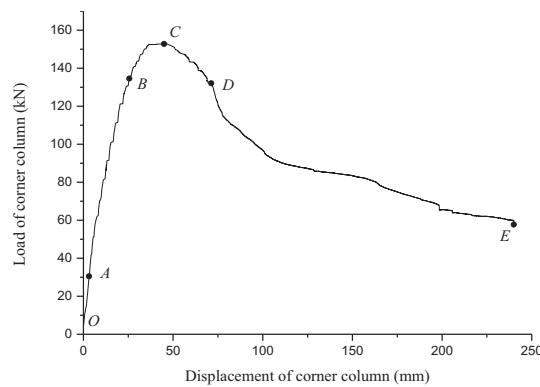


Fig. (7). Relationship between vertical load and displacement of corner column.

2.2. Collapse-resistance Mechanism

In Segment BD, it is noted that most of the steel bars at the beam ends had yielded along with the crush of concrete in the compression zones indicating the formation of plastic hinges, which implies that the frame began to sustain loads depending on the beam resisting mechanism. Fig. (8) displays the schematic diagram of the beam resisting mechanism,

in which P is the vertical load, M_{u1} and M_{u2} are the bending capacity of the plastic hinges at the beam ends. The measured force decreased gradually after the peak value at Point C and could not produce a second peak force like the phenomena of some other experiments [6, 9], which means that the catenary action did not occur in this test. It is usually believed that the catenary action could enhance the progressive collapse resistance of the structure after the failure of the beam resisting mechanism, in which all the steel bars in the beams connected to the failure joint convert to be in tension after the destruction of concrete. The tensions of steel bars increase gradually with the increasing of the rotation at the beam ends. At the large deformation stage, the structure could only depend on the tensile forces of steel bars in the beams to sustain the increasing load. To activate the catenary action, the arrangement of the steel bars in the beams should meet strict requirements, in which the steel bars need to be placed throughout the failure joint and firmly anchored at other beam-column joints. Otherwise, the steel bars will fail to be fully utilized due to steel slip.

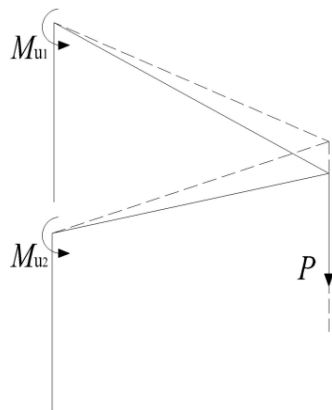


Fig. (8). Beam resisting mechanism.

In this test, the steel bars in the beams connected to the failure column were not placed throughout the joint on top of the failure corner column. Then the joint dimensions of the frame with specially shaped columns are much smaller than those of rectangular column frame. As shown in Fig. (9), the concrete at beam-column joints experienced crushing and spalling with the exposure of steel bars resulting in weak anchorage effect for steel bars. In the combined function of the above two factors, the catenary action was not generated in the test due to the weak tie force in the steel bars of beams. The variations of steel strain in beams observed in the test reveal that the compressive steel bars in the beam resisting mechanism could not completely convert to be tensile with increasing of the rotation at the beam ends, which also indicates that there would not be any catenary action to bear greater loads in latter period. Therefore, the frame sustained loads mainly depending on the beam resisting mechanism after the loss of a ground corner column and the experimental parameters related to the beam resisting mechanism have significant effects on collapse-resistance performance of the frame.



a) Joint on top of failure column



b) Joint on top of second-floor column A4

Fig. (9). Experimental details.

3. NUMERICAL ANALYSIS

3.1. Finite Element Model

OpenSees is employed to simulate the above test. The finite element model (Fig. 10) completely replicates the test, in which the properties and dimensions are identical to those in the test. The frame beam and column elements are simulated using the Force-Based Beam-Column Element from the OpenSees library [16]. Slabs are not simulated in the modeling, on which loads are applied to the adjoining beams by the rule of the two-way slab. For instance, the loads of the hatched areas are submitted to Beam A1-A2 and B2-C2 as uniformly distributed loads respectively in Fig. (11). As Sasani [17] adopted the beam elements with T-shaped or L-shaped sections to consider the enhancement of slabs on beams and achieved good agreement with test results, this kind of element section (Fig. 12) is also employed in the numerical analysis. It should be noted that the width of the effective flange is evaluated according to Chinese code for concrete structures [18].

$$b_f' = \min\left\{\frac{l_0}{3}, b + s_n, b + 12h_f'\right\} \tag{1}$$

where b_f' is the width of the effective flange, l_0 is the span of beams, b is the width of beams, s_n is the net distance between beams, and h_f' is the height of the flange. Substituting test parameters into Eqn. (1), $b_f' = 400$ is taken as the width of the effective flange.

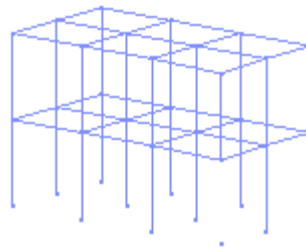


Fig. (10). Finite-element model.

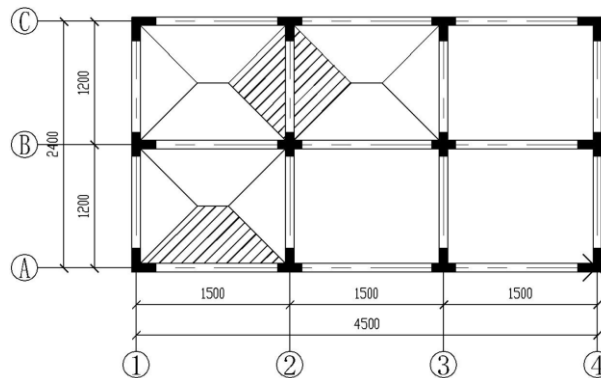


Fig. (11). Rule of the two-way slab (dimensions in mm).

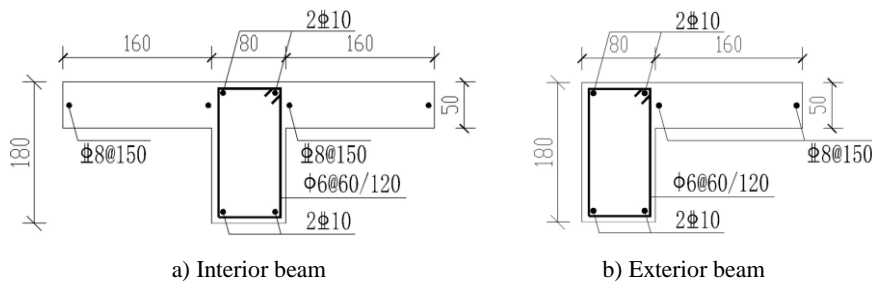


Fig. (12). Beam section considering effect of slabs (dimensions in mm).

3.2. Material Properties and Constitutive Models

The element is composed of the fiber sections in which material properties of concrete and steel bars are respectively assigned to the fibers. As displayed in Fig. (13), Hysteretic Material from OpenSees is employed herein to model steel bars. Related steel parameters in the model are summarized in Table 2. Concrete02 Material derived from the modified Kent-Park model [19] is used to describe the stress-strain relationship of concrete as shown in Fig. (14). The section of beams and columns is divided into the protective layer concrete (Unconfined Concrete) and core concrete (Confined Concrete). The ultimate compressive strain of the protective layer concrete is taken as 0.004, while the ultimate compressive strength is taken as 0 in consideration of the spalling of concrete. Related concrete parameters in the model are summarized in Table 3. The concrete strength enhancement coefficient K needs to be taken into account in the core concrete. Its constitutive equations and related parameters are defined as follows:

For rising part of the curve:

$$\sigma_c = Kf'_c \left[\frac{2\varepsilon_c}{0.002K} - \left(\frac{\varepsilon_c}{0.002K} \right)^2 \right] \tag{2}$$

For descending part of the curve:

$$\sigma_c = Kf'_c [1 - Z_m (\varepsilon_c - 0.002K)] \tag{3}$$

For horizontal part of the curve:

$$\sigma_c = 0.2Kf'_c \tag{4}$$

where K and Z_m are, respectively, the concrete strength enhancement coefficient due to stirrup constraints and the strain softening slope. They are mathematically expressed as:

$$K = 1 + \frac{\rho_s f_{yh}}{f'_c} \tag{5}$$

$$Z_m = \frac{0.5}{\frac{3 + 0.29f'_c}{145f'_c - 1000} + 0.75\rho_s \sqrt{\frac{h'}{s_h}} - 0.002K} \tag{6}$$

where f'_c is the compressive strength of concrete cylinder; f_{yh} is the yield strength of stirrup; ρ_s is the volume-stirrup ratio of beams or columns; h' is the width of core concrete; and s_h is the stirrup spacing. The ultimate compressive strain of concrete is derived as:

$$\varepsilon_{\max} = 0.004 + 0.9\rho_s \left(\frac{f_{yh}}{300} \right) \tag{7}$$

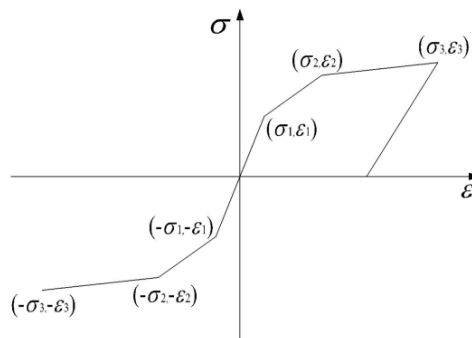


Fig. (13). Reinforcement steel constitutive model.

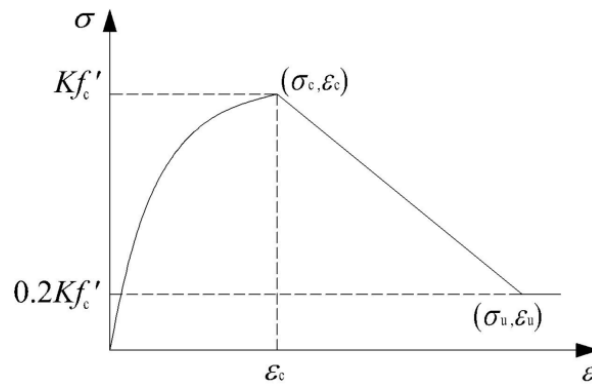


Fig. (14). Concrete constitutive model.

Table 2. Steel parameters in model.

	σ_1/MPa	ϵ_1	σ_2/MPa	ϵ_2	σ_3/MPa	ϵ_3
C8	454.1	0.01	640.3	0.02	256.1	0.25
C10	433.6	0.01	627.8	0.02	251.1	0.25

Table 3. Concrete parameters in model.

	σ_c/MPa	ϵ_c	σ_u/MPa	ϵ_u
Confined Concrete for columns	51.3	0.0031	10.3	0.0165
Confined Concrete for beams	49.5	0.0030	9.9	0.0235
Unconfined Concrete	42.3	0.0025	0	0.0040

3.3. Model Validation

The comparison between numerical and experimental results is shown in Figs. (15 and 16). As shown in Fig. (15), good agreement is achieved in the initial stiffness and behavior in the later period of the collapse stage. At the plastic-hinge stage, the simulated stiffness degrades obviously resulting in a lower peak load. It can be seen that the simulated stiffness at the early period of the collapse stage almost remains unchanged, whereas the test stiffness decreases visibly. The simulated horizontal displacements of the frame are roughly consistent with experimental results, which are compared in Fig. (16). In general, the finite element model is accurate enough to simulate the collapse process, which could provide advices for further parametric analyses.

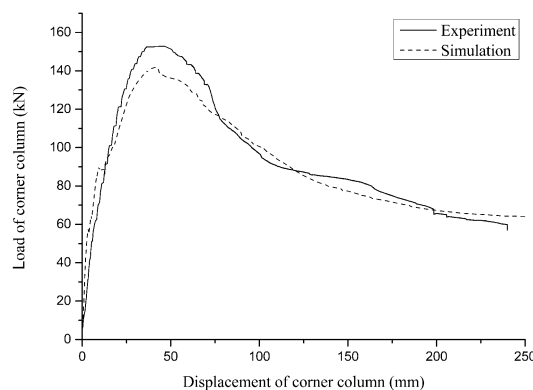


Fig. (15). Relationship between vertical load and displacement of corner column.

4. Parametric Analysis

As mentioned above, the frame sustained loads mainly depending on the beam resisting mechanism after the loss of a ground corner column. To study the factors affecting the collapse-resistance performance, four parameters related to

the beam resisting mechanism are chosen for parametric analyses which are the height of beam section (h), rebar ratio of beam (RR_b), rebar ratio of slab (RR_s) and limb length of specially shaped column (L_c).

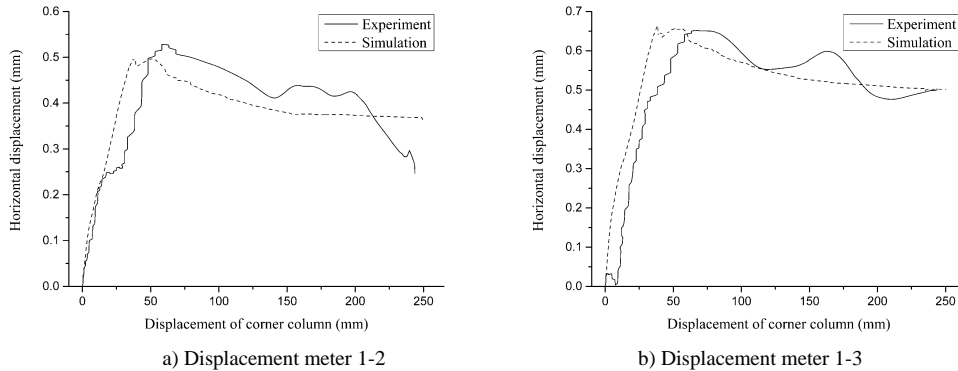


Fig. (16). Relationship between horizontal displacement and displacement of corner column.

4.1. Influence of Height of Beam Section

The height of beam section is set as 120, 180 and 240 mm (180 mm is chosen in the test) to conduct the analysis respectively. The influence of the height of beam section on collapse-resistance behavior is shown in Fig. (17). It is seen that the effect of the height of beam section on the collapse-resistance behavior of the frame is significant. The stiffness and collapse-resistance capacity remarkably increase with the increasing of the height of beam section. However, the plastic-hinge stage of the collapse process becomes shorter, which implies weaker rotation capacity of beam-column joints and ductility of the frame. The variations of horizontal displacements on top of the first-floor frame columns as a function of the vertical displacement of the failure joint are depicted in Fig. (18). With the increase of the height of beam section, the horizontal displacement increases at the measuring point 1-2 and decreases distinctly at the measuring point 1-3.

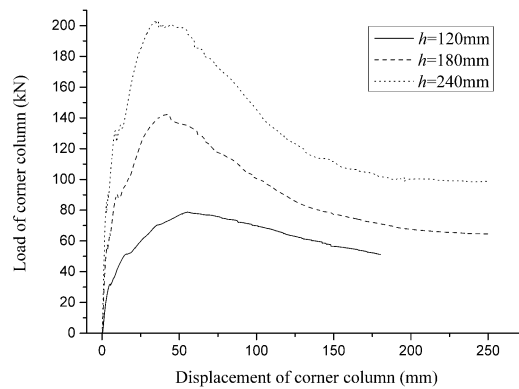


Fig. (17). Influence of height of beam section on collapse-resistance behavior.

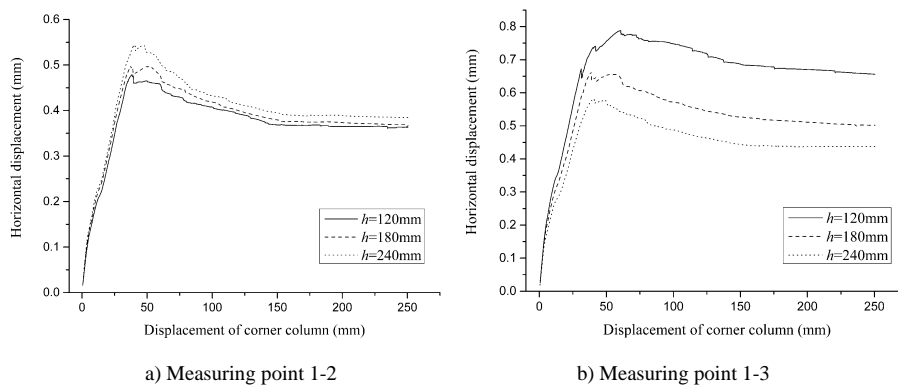


Fig. (18). Influence of height of beam section on horizontal displacement.

4.2. Influence of Rebar Ratio of Beam

The rebar ratio of the upper or lower steel bars of beam is set as 0.70%, 1.09% and 1.57% (1.09% is chosen in the test) respectively. As shown in Fig. (19a), the stiffness of the frame begins to increase in the elasto-plastic stage resulting in better collapse-resistance capacity with the increasing of the upper steel bars which serve as tensile reinforcements at the ends of beams. The lower steel bars adjacent to the failure column play an important role in the beam resisting mechanism as main tensile reinforcements. It is noted from Fig. (19b) that the growth of the lower steel bars enhances the collapse-resistance capacity significantly and lengthens the plastic-hinge stage which indicates better rotation capacity and ductility. The influences of the rebar ratio of beam on horizontal displacements of the frame are displayed in Figs. (20 and 21). Compared with the upper steel bars, the lower steel bars of beams play an important role to submit the vertical loads to other components efficiently, which improves the overall deformability of the frame. Thus, the horizontal displacements increase with the increasing of the rebar ratio of lower steel bars.

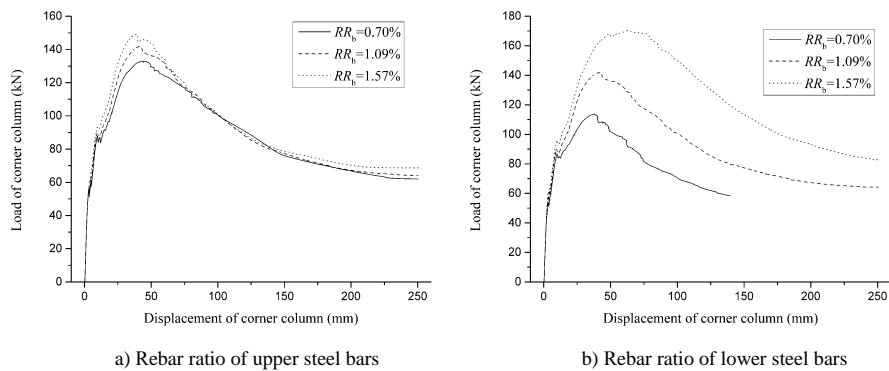


Fig. (19). Influence of rebar ratio of beam on collapse-resistance behavior.

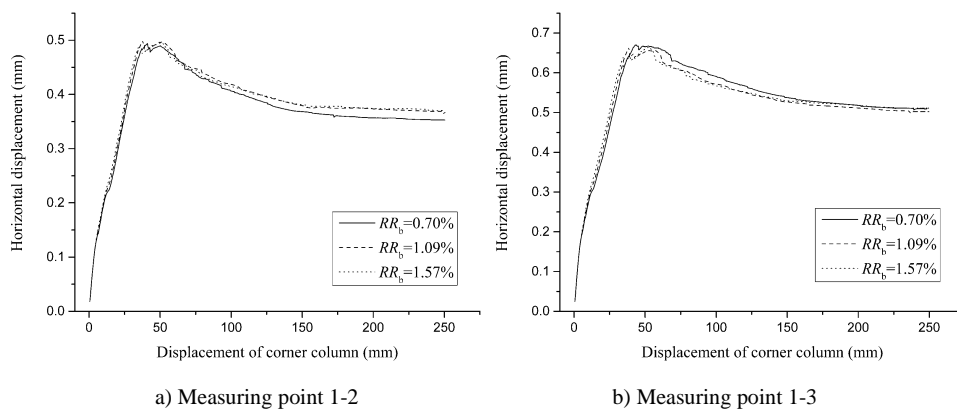


Fig. (20). Influence of rebar ratio of upper steel bars on horizontal displacement.

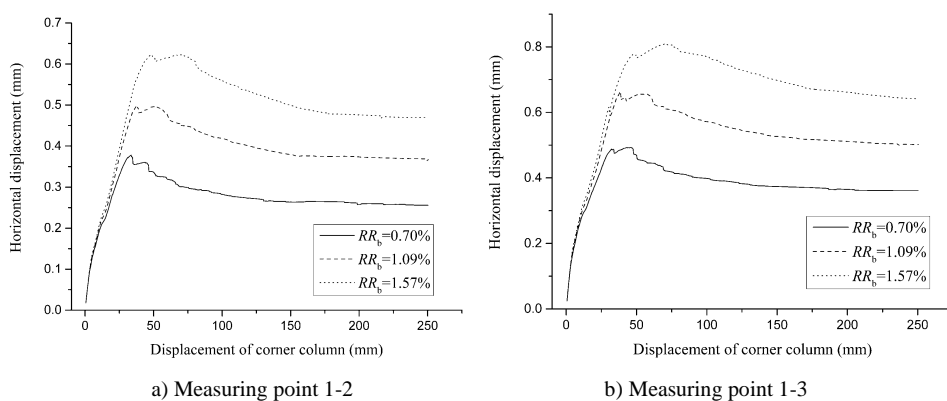


Fig. (21). Influence of rebar ratio of lower steel bars on horizontal displacement.

4.3. Influence of Rebar Ratio of Slab

The rebar ratio of slab is set as 0.38%, 0.67% and 1.05% (0.67% is chosen in the test) to conduct the analysis respectively. The steel reinforcements of slab in the range of the effective flange width are beneficial to the structural integrity and effectively participate in the beam resisting mechanism with the upper steel bars of beam at the beam ends. It can be seen from Fig. (22) that the effect of the rebar ratio of slab is similar with that of upper steel bars of beam, in which the stiffness and collapse-resistance capacity appear to increase with the increasing of the rebar ratio. The variations of horizontal displacements on top of the first-floor frame columns as a function of the vertical displacement of the failure joint are shown in Fig. (23). It is illustrated that the rebar ratio of slab has little impact on horizontal displacements of the frame, which is also similar with the results of the rebar ratio of upper steel bars of beam.

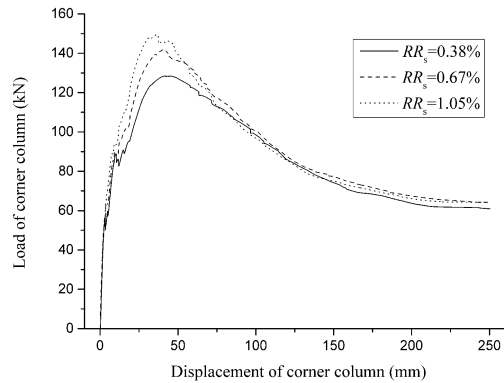


Fig. (22). Influence of rebar ratio of slab on collapse-resistance behavior.

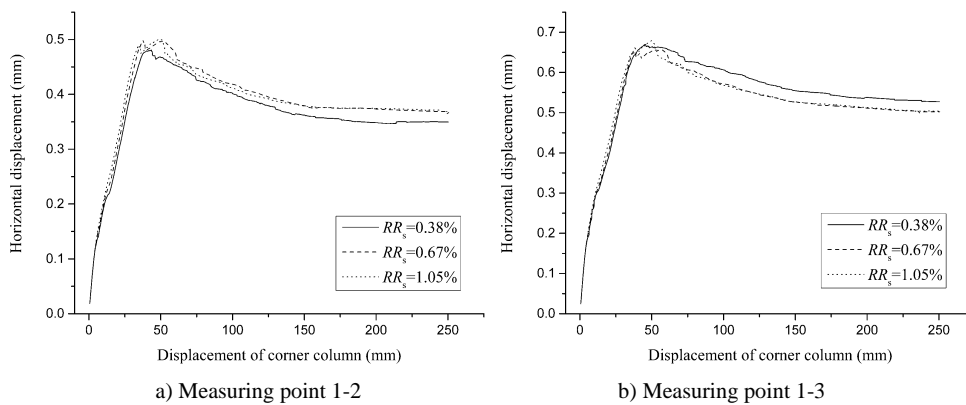


Fig. (23). Influence of rebar ratio of slab on horizontal displacement.

4.4. Influence of Limb Length of Specially Shaped Column

The limb length of specially shaped column is set as 160, 240 and 320 mm (240 mm is chosen in the test) respectively. As displayed in Fig. (24), the lengthening of the limb of specially shaped column enhances the horizontal restraining stiffness of the structure, which increases the initial stiffness but has no influence on the collapse-resistance capacity. It could be concluded that the collapse-resistance capacity of the frame with specially shaped columns following the removal of a ground corner column is mainly related to the characteristics of beams and slabs. Specially shaped columns which serve as constraint elements at the beam ends only have influence on the lateral stiffness of the frame. The influence of the limb length of specially shaped column on horizontal displacements of the frame is depicted in Fig. (25). The lengthening of the limb of specially shaped column makes shorter beam spans and stronger restraints at beam-column joints, which results in reduced out-of-plane torsion of beam sections in the collapse process of the frame. Thus, the horizontal displacements at the two measuring points reduce significantly with the increasing of the limb length of specially shaped column. In this study, the thickness of slab and rebar ratio of specially shaped column are also analyzed respectively. It is indicated that they have little influence on the collapse-resistance behavior of the frame in rational value domain.

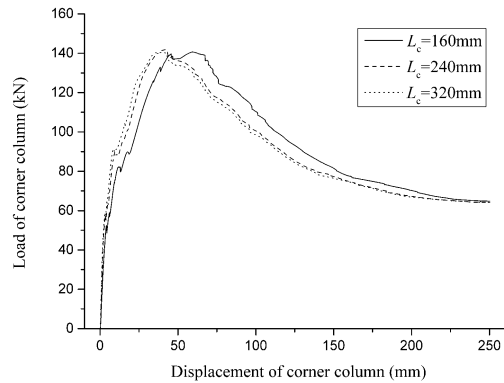


Fig. (24). Influence of limb length of specially shaped column on collapse-resistance behavior.

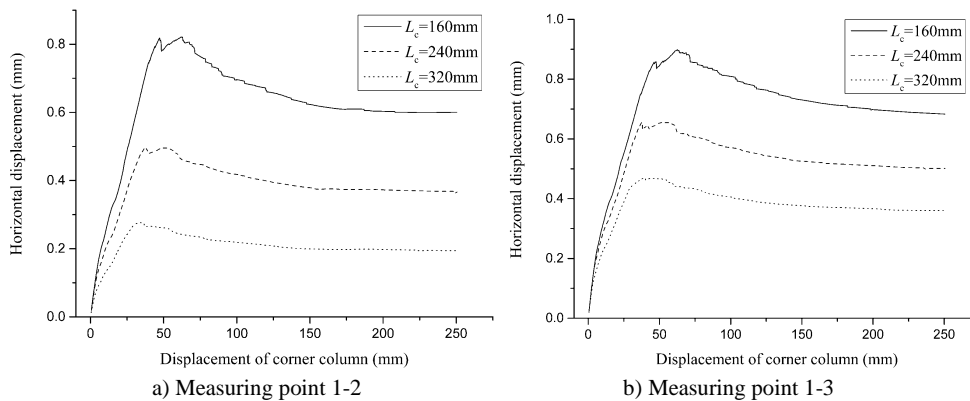


Fig. (25). Influence of limb length of specially shaped column on horizontal displacement.

5. COMPARISON WITH RECTANGULAR COLUMN FRAME

In order to satisfy the aesthetics of inhabitants and architects, the thicknesses of beams and columns of the frame with specially shaped columns are demanded to be equivalent to those of partition walls without any exposure of components out of the wall. Thus, the section of specially shaped columns could be deemed as a special form of cross section derived from cutting the section of rectangular columns along the outlines of beams and partition walls. In the light of the method herein, the sections of specially shaped columns in the test are supplemented into corresponding rectangular sections as depicted in Fig. (26) to compare the collapse-resistance performance between specially shaped column frame and rectangular column frame. The new rectangular sections should be placed at the crossing points of axes with the same column rebar ratio of longitudinal reinforcements. Thus the rectangular column frame with the column dimension of 240 mm × 240 mm is obtained to investigate its differentiation with the specially shaped column frame. The finite element analysis of the rectangular column frame is performed and the comparisons with the specially shaped column frame are shown in Figs. (27 and 28).

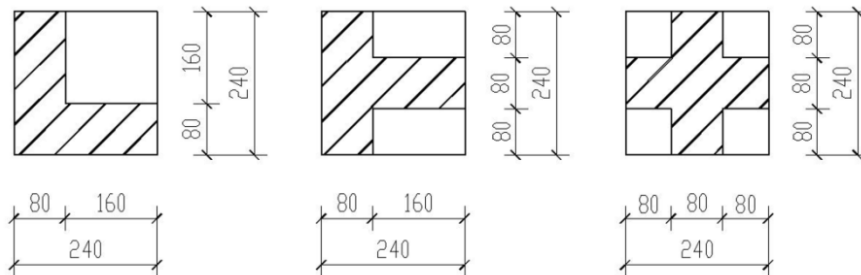


Fig. (26). Sections of rectangular and specially shaped columns (dimensions in mm).

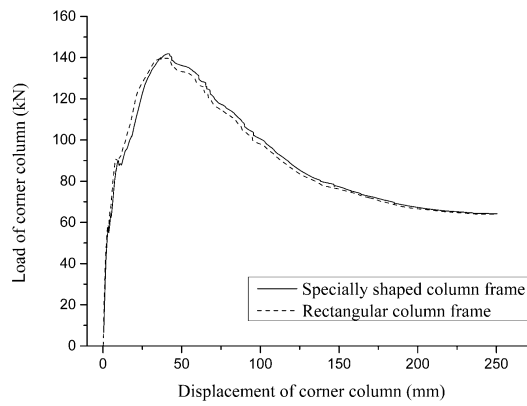


Fig. (27). Comparison of collapse-resistance behavior.

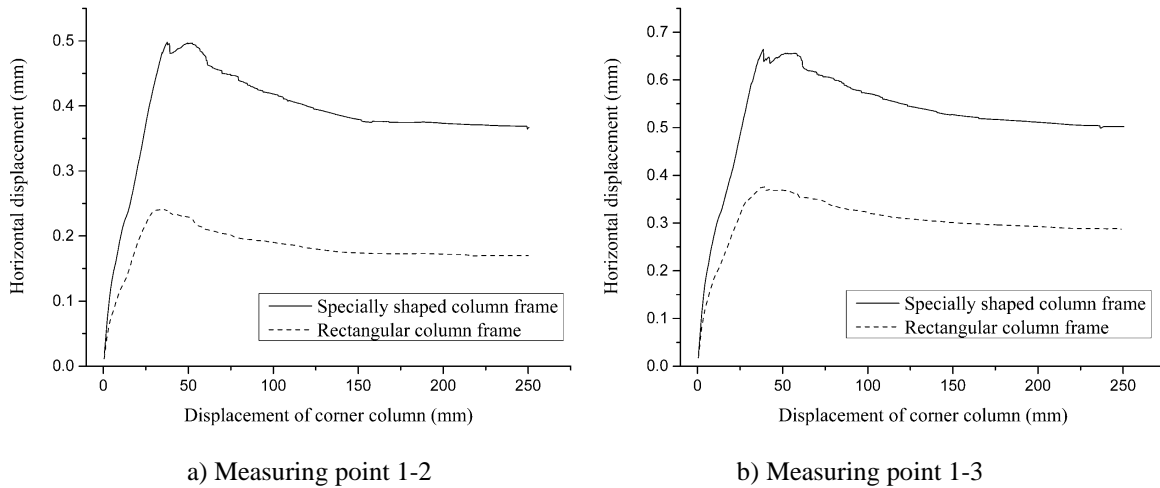


Fig. (28). Comparison of horizontal displacement.

It is seen from Fig. (27) that the stiffness of the rectangular column frame increases more fast in the elasto-plastic stage compared with the specially shaped column frame, while the collapse-resistance capacity remains nearly unchanged in the plastic hinge stage. It is turned out that the specially shaped columns merely restrict horizontal deformability of beams as vertical supporting members. It is also proved in Section 4.4 that columns only have influence on the lateral stiffness of the frame. It could be concluded that the collapse-resistance capacity of the frame with specially shaped columns under the conditions that its beam-column joints have sufficient strength and stiffness appear to be similar with the rectangular column frame. The lateral stiffness of specially shaped and rectangular column could be obtained as follows [20]:

$$D = \frac{12E_c}{h_c^3} \left(I_z - \frac{I_{yz}^2}{I_y} \right) \tag{8}$$

$$D = \frac{12E_c I_c}{h_c^3} \tag{9}$$

where I_y , I_z , and I_{yz} are the inertia moments and product of specially shaped columns sections, respectively; I_c is the inertia moment of rectangular column; h_c is the height of column; and D is the lateral stiffness of column. The section properties of different kinds of columns are summarized in Table 4. It is noted that the lateral stiffness of the specially

shaped column is smaller than that of the rectangular column under the condition of the same principal moment of inertia, which verifies the greater stiffness of the rectangular column frame in the elasto-plastic stage. As illustrated in Fig. (28), the horizontal displacements of the rectangular column frame decrease significantly at the two measuring points resulting from a greater lateral stiffness compared with the specially shaped column frame.

Table 4. Section properties of columns.

Column	A/mm^2	$I_y/10^8\text{mm}^4$	$I_z/10^8\text{mm}^4$	$I_{yz}/10^7\text{mm}^4$	$(I_x - I_{yz}^2/I_y)/10^8\text{mm}^4$	$D/(N/10^4\text{mm})$
L-shaped	32000	1.48	1.48	7.37	1.11	4.50
T-shaped	32000	0.99	1.48	0	1.48	5.98
+ -shaped	32000	0.99	0.99	0	0.99	4.00
Rectangular	57600	2.76	2.76	0	2.76	11.2

CONCLUSION

In this paper, the finite element analysis on the static test of a reinforced concrete frame with specially shaped columns in the event of one corner column removal was conducted and verified accurately enough to perform the following parametric analysis. Then the sections of specially shaped columns in the test are supplemented into corresponding rectangular sections to compare the collapse-resistance performance between specially shaped column frame and rectangular column frame. Based on the findings from the analysis described in this paper, the following conclusions can be drawn:

1. In the experiment, the catenary action was not activated in the large deformation stage as the steel bars in the beams were not placed throughout the failure joint and firmly anchored at other beam-column joints. Thus, the frame sustained loads primarily depending on the beam resisting mechanism without the effect of the catenary action. OpenSees is adopted to simulate the collapse process of the test. The simulated curves of the finite element analysis are validated in good agreement with those of the test. Therefore, the finite element model could be reliably used for further parametric analyses;

2. Four parameters related to the beam resisting mechanism are chosen for parametric analyses. It is indicated that the collapse-resistance capacity remarkably increases with the increasing of the height of beam section and rebar ratio of the lower steel bars of beam. The increase of the rebar ratio of slab and upper steel bars of beam could enhance the stiffness and collapse-resistance capacity slightly. The lengthening of the limb of specially shaped column increases the initial stiffness but has little influence on the collapse-resistance capacity. It is revealed that the rebar ratio of the lower steel bars and limb length of specially shaped column have significantly impact on the horizontal displacements of the frame; and

3. In the light of the equivalent method mentioned in the paper, the rectangular column frame is obtained to compare with the specially shaped column frame. As the columns served as vertical supporting members contribute little to the collapse-resistance capacity dominated by the beam resisting mechanism, the collapse-resistance capacities of the two frames remain nearly the same. It is noted that the lateral stiffness of the specially shaped column frame is smaller than that of the rectangular column frame, which results in larger horizontal displacements. It is concluded that the frame with specially shaped columns could maintain the equivalent collapse-resistance capacity while reduce the lateral stiffness compared with the rectangular column frame.

CONFLICT OF INTEREST

The authors confirm that this article content has no conflict of interest.

ACKNOWLEDGEMENTS

The work presented in this paper was funded by the National Natural Science Foundation of China (No. 51178304), the Special Research Foundation of Doctor Station in Chinese University (No. 20120032120055) and Application Base and Advanced Technology Research (Youth Foundation) (No. 12JCQJJC05000), which are gratefully acknowledged.

REFERENCES

- [1] ASCE 7-05. *Minimum design loads for buildings and other structures.*, American Society of Civil Engineers: Reston, VA, USA, 2005.
- [2] *Progressive collapse analysis and design guidelines for new federal office buildings and major modernization projects.*, United States General Services Administration: Washington, DC, USA, 2003.

- [3] *UFC 4-023-03. Design of structures to resist progressive collapse.*, Department of Defense: Washington, DC, USA, 2010.
- [4] M. Sasani, M. Bazan, and S. Sagioglu, "Experimental and analytical progressive collapse evaluation of actual reinforced concrete structure", *ACI Struct. J.*, vol. 104, pp. 731-739, 2007.
- [5] B.A. Izzuddin, A.G. Vlassis, A.Y. Elghazouli, and D.A. Nethercot, "Progressive collapse of multi-storey buildings due to sudden column loss - Part I: Simplified assessment framework", *Eng. Struct.*, vol. 30, pp. 1308-1318, 2008. [<http://dx.doi.org/10.1016/j.engstruct.2007.07.011>]
- [6] W.-J. Yi, Q.-F. He, Y. Xiao, and S.K. Kunnath, "Experimental study on progressive collapse-resistant behavior of reinforced concrete frame structures", *ACI Struct. J.*, vol. 105, pp. 433-439, 2008.
- [7] Y.P. Su, Y. Tian, and X.S. Song, "Progressive collapse resistance of axially-restrained frame beams", *ACI Struct. J.*, vol. 106, pp. 600-607, 2009.
- [8] H.S. Lew, J.A. Main, S.D. Robert, F. Sadek, and V.P. Chiarito, "Performance of steel moment connections under a column removal scenario. I: Experiments", *J. Struct. Eng.*, vol. 139, pp. 98-107, 2013. [[http://dx.doi.org/10.1061/\(ASCE\)ST.1943-541X.0000618](http://dx.doi.org/10.1061/(ASCE)ST.1943-541X.0000618)]
- [9] L.H. Guo, S. Gao, F. Fu, and Y.Y. Wang, "Experimental study and numerical analysis of progressive collapse resistance of composite frames", *J. Construct. Steel Res.*, vol. 89, pp. 236-251, 2013. [<http://dx.doi.org/10.1016/j.jcsr.2013.07.006>]
- [10] A. Rahai, M.S. Asghshahr, M. Banazadeh, and H. Kazem, "Progressive collapse assessment of rc structures under instantaneous and gradual removal of columns", *Adv. Struct. Eng.*, vol. 16, pp. 1671-1682, 2013. [<http://dx.doi.org/10.1260/1369-4332.16.10.1671>]
- [11] Y. Xiao, Y.B. Zhao, F.W. Li, S. Kunnath, and H.S. Lew, "Collapse test of a 3-story half-scale RC frame structure", In: *Structures Congress 2013: Bridging Your Passion with Your Profession*, 2013, pp. 11-19. Pittsburgh, PA, United states. [<http://dx.doi.org/10.1061/9780784412848.002>]
- [12] T.C. Wang, L. Zhang, H.L. Zhao, and Q.W. Chen, "Analysis on dynamic response of reinforced concrete frame for resisting progressive collapse", *Open Constr. Build. Technol. J.*, vol. 10, pp. 27-38, 2016. [<http://dx.doi.org/10.2174/1874836801610010027>]
- [13] F. Palmisano, "Mitigation of progressive collapse by the activation of the elasto-plastic catenary behaviour of R.C. slab structures", *Open Constr. Build. Technol. J.*, vol. 8, pp. 122-131, 2014. [<http://dx.doi.org/10.2174/1874836801408010122>]
- [14] T.C. Wang, L. Zhang, H.L. Zhao, and Q.W. Chen, "Progressive collapse resistance of reinforced-concrete frames with specially shaped columns under loss of a corner column", *Mag. Concr. Res.*, vol. 68, pp. 435-449, 2016. [<http://dx.doi.org/10.1680/jmacr.15.00108>]
- [15] T.C. Wang, Q.W. Chen, H.L. Zhao, and L. Zhang, *Experimental Study on Progressive Collapse Performance of Frame with Specially Shaped Columns Subjected to Middle Column Removal.*, Shock And Vibration, 2016.
- [16] *Pacific Earthquake Engineering Research Center, University of California, California, USA, 2002.* Available from: (<http://opensees.berkeley.edu>)
- [17] M. Sasani, "Response of a reinforced concrete infilled-frame structure to removal of two adjacent columns", *Eng. Struct.*, vol. 30, pp. 2478-2491, 2008. [<http://dx.doi.org/10.1016/j.engstruct.2008.01.019>]
- [18] *GB50010-2010. Code for Design of Concrete Structures.*, Publishing House of Building Industry: Beijing, China, 2010.
- [19] B.D. Scott, R. Park, and M.J. Priestley, "Stress-strain behavior of concrete confined by overlapping hoops at low and high strain rates", *ACI J. Proc.*, vol. 79, pp. 13-27, 1982.
- [20] J.H. Sun, W.J. Lou, G. Gan, and J.C. Tang, "Study on lateral stiffness of special shaped column structure", *J. Shenyang Jianzhu Univ.*, vol. 25, pp. 635-639, 2009. [Natural Science].